Electrical and Infrared Properties of Thin Niobium Microbolometers near T_c

E.N. Grossman, J.E. Sauvageau, and D.G. McDonald

Electromagnetic Technology Division
National Institute of Standards and Technology
Boulder, CO

S53-33
160567
N93-27779

Abstract

Niobium microbolometers approximately 1 μm wide × 2 μm long × 10 nm thick have been integrated at the feeds of equiangular spiral antennas made of 200 nm thick Nb. The device's current-voltage characteristic and infrared responsivity as a function of DC bias voltage were measured over a range of temperature spanning approximately ± 2 % around T_c. The greatest voltage responsivity occurs well below T_c, in a regime where the I-V curve is significantly hysteretic due to self-heating and resembles the I-V curve of a superconducting microbridge.

The idea of constructing sensitive terahertz-frequency bolometers by combining the principle of antenna-coupling with that of superconducting transition-edge thermometry has recently received much attention[1,2]. The idea is to use a lithographic antenna to concentrate the infrared power into an area much smaller than a square wavelength. At the feed of the antenna are integrated both an absorbing load (simply a film that is conjugately matched to the antenna impedance at the IR frequency), and a superconducting transition-edge thermometer, used to monitor the changes in the absorber's temperature as varying IR powers are applied to it. The absorber and the thermometer can physically be the same thin-film device, since at IR frequencies, well above the superconductor's gap frequency, its impedance is just that of the normal metal. The device is temperature-biased at the midpoint of the thermometer's resistive transition. A small bias current is applied to it and its resistance changes monitored by measuring the voltage developed across it. Previous analyses of these devices have electrically modelled the thermometer in a very simple way, namely as a lumped (i.e. spatially homogeneous) temperature-dependent ohmic resistance. That is, it has been assumed that near T_c the temperature and current dependent voltage may be separated as $V(I,T) = IR(T)$. This method of analysis naturally grew out of earlier, quite successful, work[3] on large area, surface-absorbing bolometers. However, there is some reason to expect that very small bolometers may behave differently from large ones. In particular, as the superconducting transition temperature is approached from below, ($1 - t \to 0$, where $t = T/T_c$), both the London penetration depth and the Ginzburg-Landau coherence length diverge, as $(1 - t)^{-1/2}$. At quite realistic values of $(1-t)$, one or both length scales may become comparable to or larger than the lateral dimensions of a small bolometer at the feed of a lithographic microantenna. This can create qualitatively new physical effects. For example, if the bolometer is comparable in width to the penetration depth, flux flow conduction is strongly affected because the current distribution due to a single magnetic vortex is highly perturbed by the bolometer edges. If the the bolometer is comparable in size to the coherence length, a weak link, or localized region of depressed superconductivity, is created. Such finite-size effects have been recognized for a long time[4] as important to the the electrical properties of small microbridges near T_c.

Another method of creating a superconducting microbolometer is to monitor the temperature-induced change in the thermometer's inductance[5,6]. The inductance change is due to the variation in the pentration depth with temperature discussed above, and is not confined to a very narrow range of temperature near T_c. Such an inductive thermometer can be formed from exactly the same physical device as the resistive thermometer, namely a thin superconducting film patterned so as to contact and span the two antenna terminals. Aside from not requiring such precise temperature control as a transition-edge bolometer, operating well below T_c with an inductive thermometer allows the existence of a large population of unbroken Cooper pairs, which provides a separate, non-thermal mechanism for far-infrared detection, namely direct pair-breaking. Previous work[7] has indicated that this mechanism can be much faster than bolometric detection, at least in hard superconductors, such as niobium. Our research on such photoinductive detectors relies on the use of an integrated DC SQUID (superconducting quantum interference device) to convert changes in the device's inductance to measurable voltage changes. Unfortunately, we have not yet succeeded in reliably fabricating a DC SQUID integrated with a photoinductive film and a lithographic antenna. We have therefore investigated some of the properties of the thin detectors near T_c, where the resistive mode of operation obviates the need for a SQUID.

The devices consist of pure niobium films 10 nm thick, patterned by conventional optical lithography into bolometers nominally 1 μm wide by 2 μm long. The bolometer lies at the feed of a self-complementary spiral antenna with a 65° opening angle, formed from 200 nm thick niobium. (See figure 1.) Reliable, low resistance electrical contact between the antenna feed and the thin bolometer is accomplished by DC magnetron sputtering the two films successively, with an Al etch-stop layer between them, in a single deposition run, without breaking vacuum. The antenna, etch-stop layer, and bolometer are then patterned by a sequence of plasma and wet etches. At low temperatures, the thin (10 nm) Al etch stop layer is rendered superconducting by the proximity effect from the much thicker Nb antenna lying on top of it, and can therefore be neglected electrically. The DC normal-state resistance of the bolometers is approximately 20 Ω. At frequencies well above the Nb energy gap frequency $2\Delta/h \approx 700$ GHz, but well below the normal electron relaxation frequency $v_F/l_e = 48$ THz[8], the impedance of the bolometer, both above and below T_c, should approximate the DC normal-state resistance. (v_F is the Fermi velocity and l_e the electronic mean free path.) This implies a loss of about 1.8 dB due to impedance mismatch with the antenna, if the antenna impedance can be approximated by the quasi-static value of about 75 Ω appropriate to a self-complementary design on a silicon substrate.

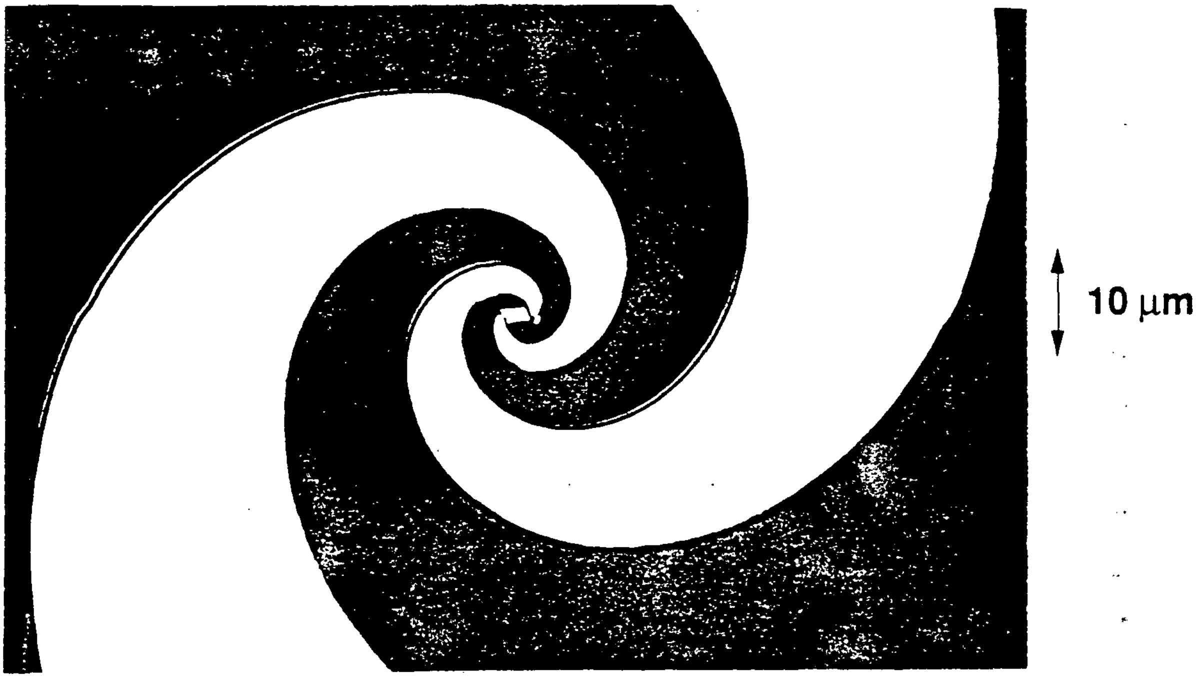

Figure 1. Photograph of the antenna-coupled microbolometer

The diced chips, 1 cm square, were placed circuit-side up against a Si hemisphere, and the infrared radiation coupled in through the hemisphere and substrate, in the conventional "reverse microscope" configuration[9]. Mechanical pressure was applied from the circuit side to hold the chip in place against the hemisphere and to maintain an optical quality contact between the polished Si surfaces of the substrate and hemisphere. The very wide antenna beam[1]0 was refocussed by an off-axis elliptical mirror operating at an angular magnification of 6.3 to a point inside the cryostat where a cold field stop was placed to reduce to a manageable level the total background power incident on the chip (i.e. the power in spatial modes other than the one coupled to the antenna).

This is necessary because the hemisphere/chip assembly is mounted on a thermal platform whose thermal resistance to the heat bath is fairly high in order to allow convenient temperature regulation and control. Any substantial optical background power would therefore raise the platform's (and chip's) temperature excessively. The refocussed beam from the elliptical mirror is then collimated by a cold lens before emerging through the cryostat window. (See figure 2.) The material of the collimating lens may be chosen to define a broad spectral bandpass and optical power level that is desired. In the optical measurements described here, a ZnSe lens was used to define a broad, short wavelength ($\lambda < 20$ μm) bandpass. The optical input was mechanically chopped between simple blackbody sources at 300 K and 77 K. Using handbook values[11] for the transmission of Si and ZnSe, the power coupled into the single spatial mode of the antenna is calculated from $P = \frac{(kT)^2}{h}\int_0^\infty \frac{xT(x)dx}{e^x-1}$, where $x = h\nu/kT$ is the dimensionless frequency, h is Planck's constant, k Boltzmann's constant, $T(x)$ the transmittance of the combination of Si and ZnSe lenses, and T the absolute temperature. This yields a power difference $P(300K) - P(77K) = 1.86$ nW. When the reflection losses at the surfaces of the ZnSe and Si lenses and the KRS-5 cryostat window are included, a total incident optical signal power of 0.65 nW is obtained. The power-weighted mean frequency of the optical input is 28 THz (wavelength 11 μm).

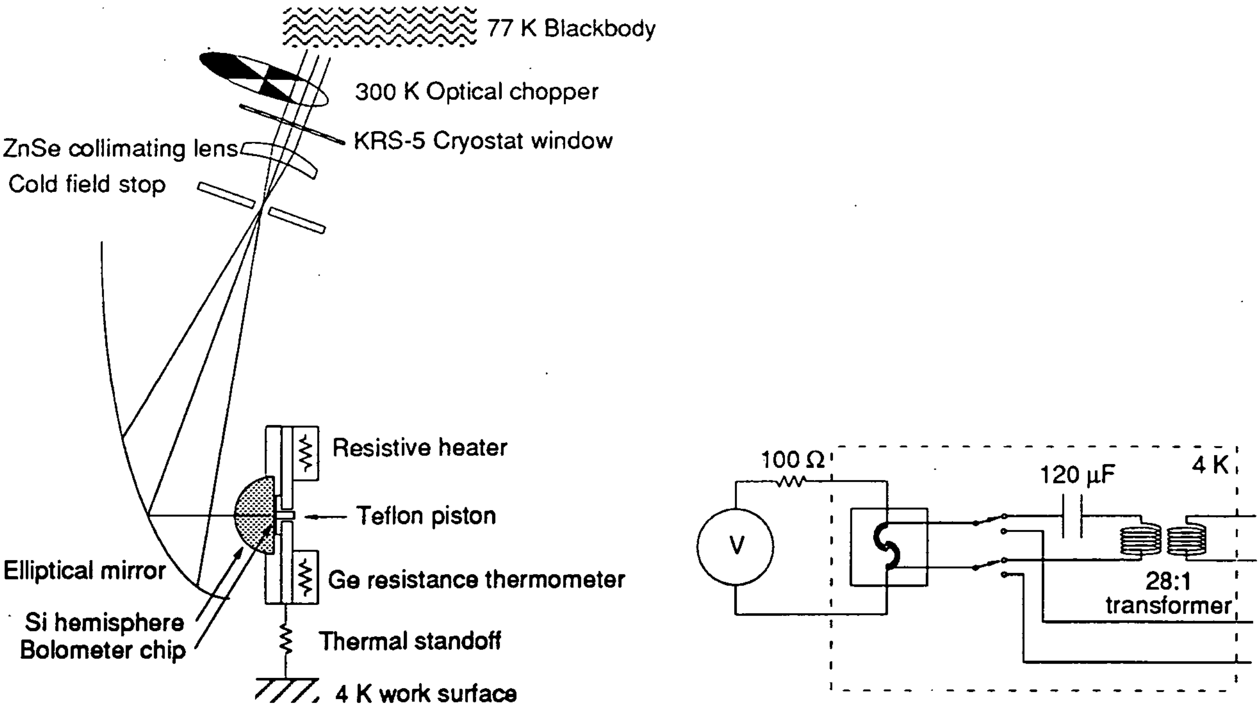
77 K Blackbody
300 K Optical chopper
KRS-5 Cryostat window
ZnSe collimating lens
Cold field stop
Resistive heater
Teflon piston
Ge resistance thermometer
Elliptical mirror
Si hemisphere
Bolometer chip
Thermal standoff
4 K work surface
100 Ω
V
120 μF
4 K
28:1
transformer

Figure 2. Experimental setup for the infrared responsivity measurements

The device was electrically biased through the antenna arms by a 100 Ω output impedance source. The voltage was monitored (in a 4-terminal configuration) at the outer periphery of the antenna arms. Since the antenna is formed of much thicker Nb than the bolometer, the critical temperature of the antenna arms is some 0.8 K higher than that of the bolometer. Therefore, over the entire temperature range investigated, the antenna arms formed (at DC and audio frequencies) a superconducting short circuit, and the measured voltage was just that across the bolometer element itself. As shown in figure 2, a cold transformer, separately calibrated at 4 K, could be switched into the circuit to raise the signal voltage level and improve the match to the high impedance room temperature amplifier which followed. To obtain high sensitivity from a small superconducting detector (i.e. one which is not a long meander line), it is essential to provide such an impedance transformation. In many cases, however, we did not use the transformer in order to avoid certain ambiguities in interpretation of the data. For example, it turned out that the bias-dependent dynamic impedance of the device varied over a huge range; at its highest values, the RC rolloff frequency created between the post-transformer device impedance and the filter capacitance on the signal lines became comparable with the optical chopping frequencies (10 - 400 Hz). Obviously, this would cause spurious systematic structure in the curve of optical response versus bias, which was avoided by measuring the voltage before the transformer, where the signal impedance is much lower.

The basic data consist of curves of demodulated optical signal voltage and DC current versus DC bias voltage, obtained at various temperatures above and below the superconducting transition. (Since the dynamic impedance of the device is frequently comparable to the 100 Ω bias source impedance, the choice between DC voltage and current as the independent variable is more or less arbitrary.) The set of data with the most complete temperature coverage is shown in figure 3. It was taken with the cold transformer switched out of the circuit. As the DC voltage was slowly swept, the DC current and demodulated optical signal were recorded simultaneously. During all the measurements, the temperature of the platform was monitored with a Ge resistance thermometer and actively stabilized, with a precision of about 0.2 mK, by a commercial temperature controller driving a simple resistive heater. The critical temperature of the bolometer as defined by the onset of a supercurrent (i.e. vanishing zero-voltage resistance) was 7.978 ± .006 K. The critical temperature as defined by a zero-voltage resistance that is half the normal state resistance was 7.992 ± .010 K. The data cover a range in reduced temperature from about 2.4 % below to +2.2 % above the critical temperature, a much wider range than envisaged for "transition-edge" bolometers in the previous analyses[1,2].

The most obvious feature of the data is the huge increase in infrared responsivity at low voltage

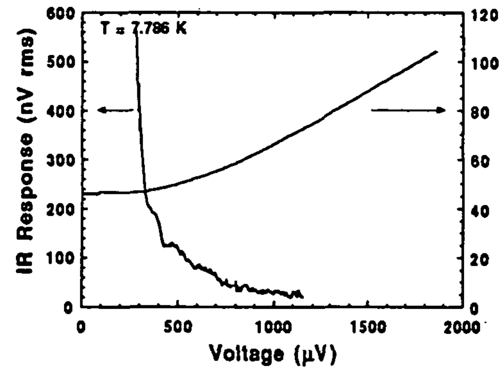
T = 7.786 K
IR Response (nV rms)
Current (μA)
Voltage (μV)
0
100
200
300
400
500
600
0
20
40
60
80
100
120
0
500
1000
1500
2000

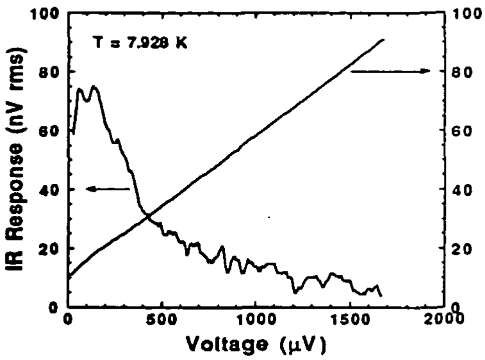
T = 7.928 K
IR Response (nV rms)
Current (μA)
Voltage (μV)
0
20
40
60
80
100
0
20
40
60
80
100
0
500
1000
1500
2000

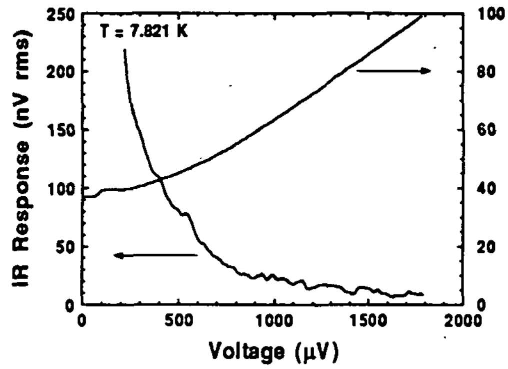
T = 7.821 K
IR Response (nV rms)
Current (μA)
Voltage (μV)
0
50
100
150
200
250
0
20
40
60
80
100
0
500
1000
1500
2000

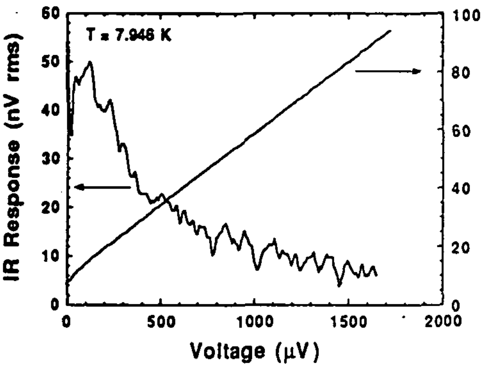
T = 7.946 K
IR Response (nV rms)
Current (μA)
Voltage (μV)
0
10
20
30
40
50
60
0
20
40
60
80
100
0
500
1000
1500
2000

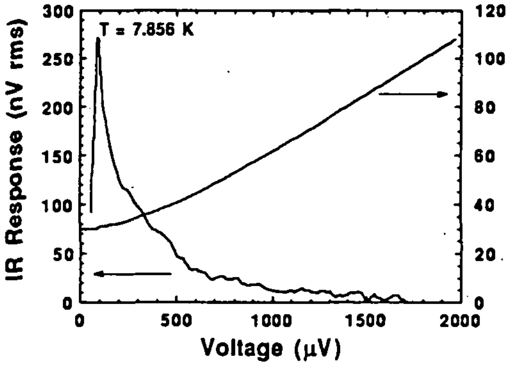
T = 7.856 K
IR Response (nV rms)
Current (μA)
Voltage (μV)
0
50
100
150
200
250
300
0
20
40
60
80
100
120
0
500
1000
1500
2000

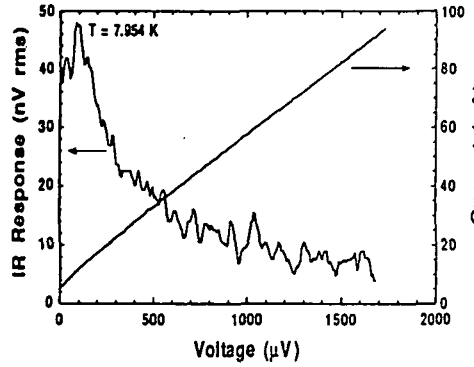
T = 7.954 K
IR Response (nV rms)
Current (μA)
Voltage (μV)
0
10
20
30
40
50
0
20
40
60
80
100
0
500
1000
1500
2000

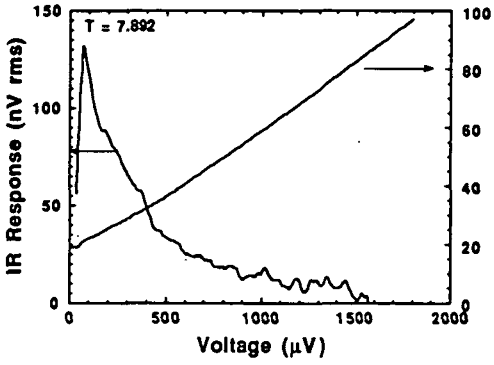
T = 7.892
IR Response (nV rms)
Current (μA)
Voltage (μV)
0
50
100
150
0
20
40
60
80
100
0
500
1000
1500
2000

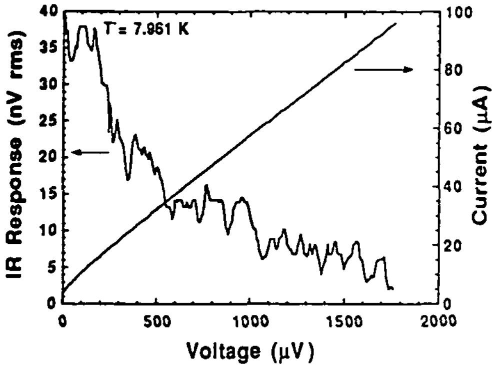
T = 7.961 K
IR Response (nV rms)
Current (μA)
Voltage (μV)
0
5
10
15
20
25
30
35
40
0
20
40
60
80
100
0
500
1000
1500
2000

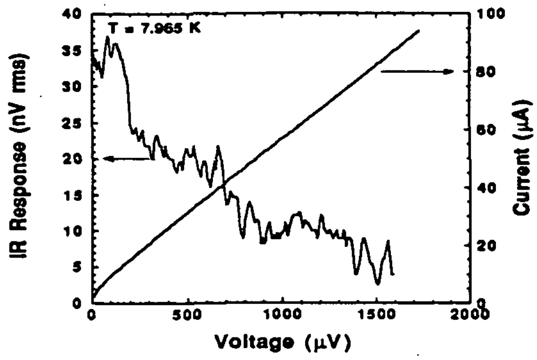
T = 7.965 K
IR Response (nV rms)
Current (μA)
Voltage (μV)
0
5
10
15
20
25
30
35
40
0
500
1000
1500
2000
0
20
40
60
80
100

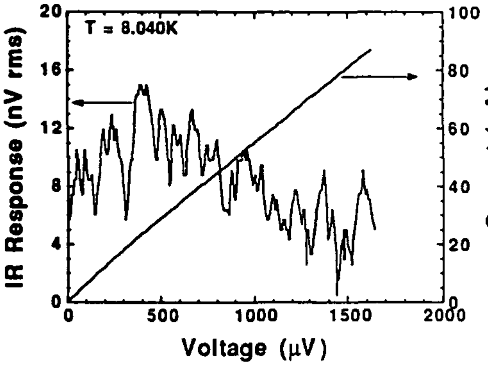
T = 8.040K
IR Response (nV rms)
Current (μA)
Voltage (μV)
0
4
8
12
16
20
0
500
1000
1500
2000
0
20
40
60
80
100

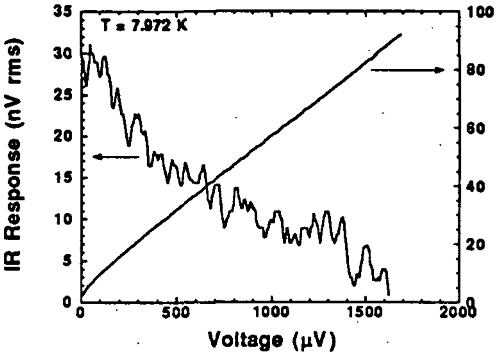
T = 7.972 K
IR Response (nV rms)
Current (μA)
Voltage (μV)
0
5
10
15
20
25
30
35
0
500
1000
1500
2000
0
20
40
60
80
100

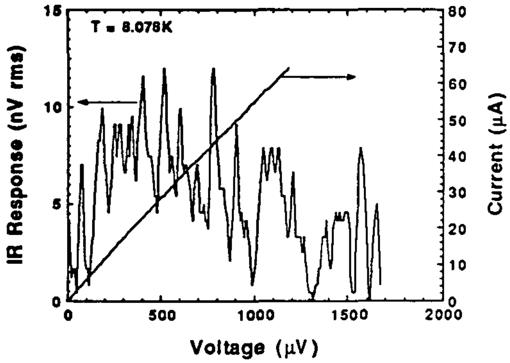
T = 8.078K
IR Response (nV rms)
Current (μA)
Voltage (μV)
0
5
10
15
0
500
1000
1500
2000
0
10
20
30
40
50
60
70
80

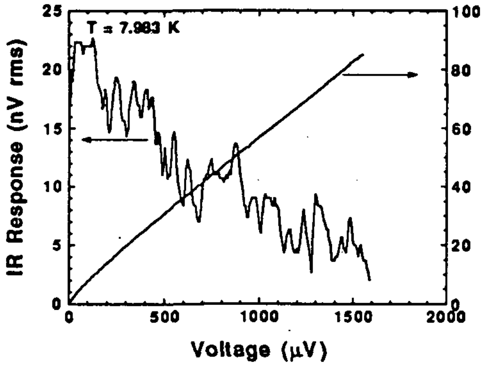
T = 7.983 K
IR Response (nV rms)
Current (μA)
Voltage (μV)
0
5
10
15
20
25
0
500
1000
1500
2000
0
20
40
60
80
100

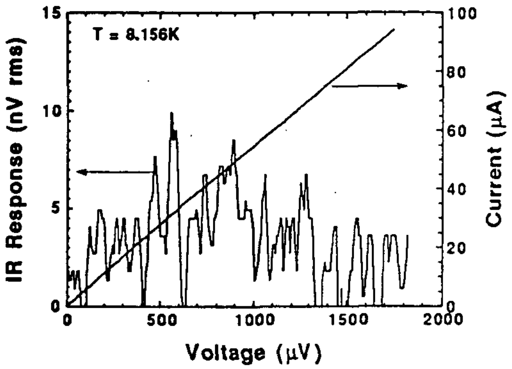
T = 8.156K
IR Response (nV rms)
Current (μA)
Voltage (μV)
0
5
10
15
0
500
1000
1500
2000
0
20
40
60
80
100

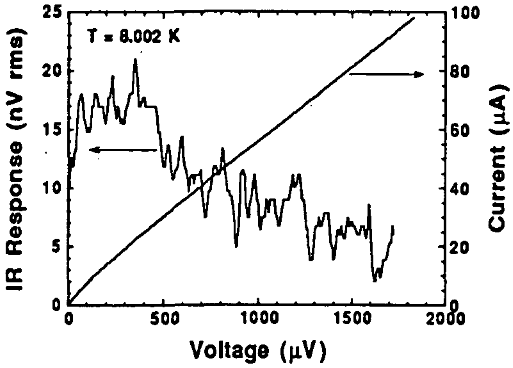
T = 8.002 K
IR Response (nV rms)
Current (μA)
Voltage (μV)
0
5
10
15
20
25
0
500
1000
1500
2000
0
20
40
60
80
100

and low temperature. (Note the changes in scale of the IR response from graph to graph in figure 3.) This is partly due to the fact that, with a 100 Ω load line (nearly a current source on the scale of the figure) and voltage detection, the largest infrared signals will be obtained where the device's dynamic impedance is the greatest. Thus, for the graphs at $T \leq 7.856\ K$, the large increase in infrared responsivity corresponds with a large increase in dV/dI at $V \leq 1000\ \mu$V. Indeed, at these low temperatures, both the dynamic impedance and the IR responsivity apparently diverge as the bias approaches the point of instantaneous "dropback" to the zero-voltage branch. As this point is approached, it becomes increasingly difficult to bias the device stably. In these measurements, bias stability appears to be the practical limitation on increasing the responsivity by this means. At temperatures T ≤ 7.892 K, the I-V curve is hysteretic, undoubtedly due to ohmic self-heating (see below). Only the descending branch is plotted in fig. 3. For T = 7.892 K and 7.856 K, the hysteresis loop encloses only the small horizontal "step" visible at $V \leq 100\mu$V in the I-V curve, while at lower temperatures, the difference between the critical current (on the ascending branch) and the "dropback" current increases.

The data of figure 3 broadly describes the behavior of the IR responsivity over a large area in parameter space, the "big picture", but it does not give a very accurate idea of the responsivity in the region of optimum device performance. Other data we have taken exhibit much higher responsivities than those of figure 3; values as high as 4.8×10^4 V/W after the transformer and 7800 V/W before the transformer have been measured. Even these figures do not really reflect the device's capabilities, however, since the test conditions were not optimum for the unexpectedly high device impedances in this operating range. Firstly, the capacitance values for the cold blocking capacitor and the cryostat feedthru capacitors turned out to be inappropriate for attaining the full advantage of the transformer, and secondly, the operating temperature was not varied over a fine enough grid to find the optimum operating point of the bare bolometer. Nonetheless, these responsivity figures in themselves demonstrate technologically interesting levels of sensitivity for the bolometer.

The device's dynamic impedance cannot provide the entire explanation for the observed dependence of IR responsivity on bias visible in figure 3. This is clear from the data at $T \geq 7.928\ K$, where the dynamic impedance increases at *higher* bias voltages, yet the strong increase in IR responsivity at low voltage persists. An effect which certainly must be important in understanding this data is local ohmic heating. This creates temperature gradients on the chip, in the immediate vicinity of the bolometer, which of course are not probed or regulated by the Ge thermometer and temperature control unit mounted on the thermal platform. At the biases typical in figure 3, this is the dominant effect, since the ohmic heating powers are in the range of tens of nW, which translates into hundreds of mK temperature rise, for typical thermal conductances of 1-5 $\times 10^{-7}$ W/K[12].

In the previous treatments of superconducting microbolometer performance[1,2], ohmic heating is incorporated by assuming the bolometer itself remains isothermal, (i.e. by ignoring any spatial temperature gradients across the bolometer) and by imposing a condition on the DC bias, that $\frac{dR}{dT}\frac{I_{bias}^2}{G} < 1$, where G is the thermal conductance of the bolometer to the heat bath. As long as this condition for avoiding thermal runaway is met, the device is treated as ohmic, with a temperature dependent resistance, implying that $dV/dT = V\frac{d(ln(R))}{dT}$ and the infrared responsivity should be linearly proportional to DC voltage. The regime in which this treatment is valid covers a small region near the origin of the graphs for $T \geq 7.98$ K.

For the regime at lower temperature, where the measured infrared responsivity is higher, an apparently more appropriate treatment is that developed by Skocpol, Beasley, and Tinkham[13,14] to describe self-heating effects and phase-slip centers in microbridges (see figure 7 in ref. 13 for example). This model explicitly includes spatial temperature gradients. In fact, it assumes that in general, part of the bridge can be normal and part superconducting. The voltage across the bridge at any particular substrate temperature and bias current is determined by the length of the region where $T > T_c$, which is in turn determined by a self-consistent balance between the ohmic heat generated in that region and the power conducted away from it, which depends on the geometry. Well below T_c, there is strong non-linearity in the I-V curve above the critical current due to the rapidly changing size of the normal region of the bridge. Presumably, the large infrared response we see in our devices well below T_c is due to the IR power, dissipated approximately uniformly across the bolometer's surface area, changing the thermal balance in such way as to move the boundary between the bolometer's normal and superconducting regions. Very small changes in IR power apparently move this boundary very far. In some sense, the ohmic heating due to the bias current adds some positive feedback to the process of driving the bridge normal with infrared heating.

Unfortunately, the theoretical results described in reference 13 cannot be directly applied to our devices because of a difference in length scales. The microbridges discussed there, which were fabricated mechanically rather than lithographically, were in general substantially larger than our devices. On the other hand, the characteristic length scale which figures into their model is the quasiparticle diffusion length. The devices in that study were formed of tin, a soft superconductor with a much larger diffusion length than niobium. Therefore, it is very likely on theoretical grounds that our devices can in fact be treated by that model, appropriately rescaled. More specific statements, however, including any theoretical estimate of the optimal infrared responsivity available from this mechanism, must await the results of quantitative modeling.

In conclusion, we have measured the infrared responsivity of antenna-coupled, superconducting microbolometers as a function of DC bias and temperature, over a wider range than has been envisaged in previous theoretical treatments. We find the highest responsivity occurs in a regime well below T_c, where the effects of ohmic heating due to the bias current are of dominant importance. A model developed to describe self-heating and phase slip centers in tin microbridges may provide the most appropriate framework for analyzing the device's infrared response and electrical properties in this regime.

We are grateful to Ron Ono for bringing the microbridge self-heating model to our attention. This work was supported by the Innovative Science and Technology Agency of SDIO, and by NASA, through the Office of Space Science and Applications.

References

1. J. Mees, M. Nahum, and P.L. Richards, *Appl. Phys. Lett.*, **59**, p. 2329 (1991)

2. M. Nahum and P.L. Richards, *IEEE Trans. Magn.*, **MAG-27**, p. 2484 (1991)

3. J. Clarke, G.I. Hoffer, P.L. Richards, and N.H. Yeh, *J. Appl. Phys.*, **48**, p.4865 (1978)

4. R.D. Parks, J.M. Mochel, and L.V. Surgent, *Phys. Rev. Lett.*, **13**, p. 331a (1964)

5. D.G. McDonald, *Appl. Phys. Lett.*, **50**, p. 775 (1987)

6. E.N. Grossman, D.G. McDonald, and J.E. Sauvageau, *IEEE Trans. Magn.*, **27**, p. 2677 (1991)

7. M. Johnson, *Phys. Rev. Lett.*, **67**, p.374 (1991)

8. The electron relaxation frequency is obtained from the free-electron expression $\omega_r^2 = \frac{3\pi^2\hbar^3\sigma_0}{e^2m^2l_e^3}$, using a DC conductivity $\sigma_0(10\,K) = 1.58 \times 10^7$ m$^{-1}\Omega^{-1}$, W.H. Henkels and C.J. Kircher, *IEEE Trans. Magn.*, **MAG-13**, p. 63 (1977), and an electron mean free path $l_e = 6.3$ nm, S. Wolf, J.J Kennedy, and M. Nisenoff, *J. Vac. Sci. and Tech.*, **13**, p. 145 (1975)

9. D.B. Rutledge, D.P. Neikirk, and D. Kasilingham, chap. 1 in *Infrared and Millimeter Waves*, vol. 10, Academic Press, New York, (1983)

10. E.N. Grossman, J.E. Sauvageau, and D.G. McDonald, *Appl. Phys. Lett.*, **59**, p. 3225 (1991)

11. E.D. Palik (ed.) *Handbook of Optical Constants of Solids*, Academic Press, Orlando (1985), and

E.D. Palik (ed.) *Handbook of Optical Constants of Solids II*, Academic Press, San Diego (1991)

12. E.N. Grossman, D.G. McDonald, and J.E. Sauvageau, *Proceedings of the Second International Symposium on Space Terahertz Technology*, p. 407, JPL, Pasadena, CA (1991)

13. W.J. Skocpol, M.R. Beasley, and M. Tinkham, *J. Appl. Phys.*, **45**, p.4054 (1974)

14. W.J. Skocpol, M.R. Beasley, and M. Tinkham, *J. Low Temp. Phys.*, **16**, p. 145 (1974)